

DDOS: The Drone Depth and Obstacle Segmentation Dataset

Benedikt Kolbeinsson
Imperial College London
bk915@imperial.ac.uk

Krystian Mikolajczyk
Imperial College London
k.mikolajczyk@imperial.ac.uk

<https://huggingface.co/datasets/benediktkol/DDOS>

Abstract

Accurate depth and semantic segmentation are crucial for various computer vision tasks. However, the scarcity of annotated real-world aerial datasets poses a significant challenge for training and evaluating robust models. Additionally, the detection and segmentation of thin objects, such as wires, cables, and fences, present a critical concern for ensuring the safe operation of drones. To address these limitations, we present a novel synthetic dataset specifically designed for depth and semantic segmentation tasks in aerial views. Leveraging photo-realistic rendering techniques, our dataset provides a valuable resource for training models using a synthetic-supervision training scheme while introducing new drone-specific metrics for depth accuracy.

1. Introduction

The safe operation of drones typically requires the accurate detection and segmentation of thin objects, such as wires, cables, and fences, which can pose as dangerous obstacles. Detecting and segmenting these objects with precision is crucial for enabling efficient drone navigation and avoiding potential hazards. However, due to the fine spatial characteristics and limited representation of thin objects in existing datasets, this domain remains relatively understudied in aerial analysis [11].

Existing datasets for depth estimation and semantic segmentation in aerial imagery primarily focus on common objects like buildings, vehicles, and trees [4, 15]. While these datasets have facilitated significant progress in aerial analysis, they do not adequately address the unique challenges posed by thin objects. Thin objects often exhibit intricate and elongated structures, making them difficult to detect and accurately segment from aerial views. Moreover, the limited occurrence of thin objects in existing datasets hampers the development and evaluation of robust algorithms.

To bridge this gap, we propose the Drone Depth and Obstacle Segmentation (DDOS) dataset, a synthetic dataset specifically designed to address the scarcity of labeled real-world data and emphasize the detection and segmentation

of thin objects from aerial perspectives. DDOS leverages advanced techniques in computer graphics and rendering to generate synthetic aerial images that closely resemble real-world scenes. By incorporating photo-realistic qualities, DDOS enables the exploration of thin object detection and segmentation algorithms in a controlled environment.

The synthetic nature of DDOS offers several advantages over traditional real-world datasets. First, it provides a substantially larger and diverse set of labeled examples of thin objects, which are typically scarce in real-world scenarios. This abundance of labeled data enables more effective training and evaluation of thin object detection and segmentation algorithms. Second, by generating synthetic images, we have access to pixel-perfect ground truth annotations, depth, optical flow and surface normals, which allows for a cleaner training signal.

To facilitate a comprehensive understanding of the dataset, we conduct a detailed statistical analysis of DDOS, focusing on various key attributes such as class density, flight characteristics and spatial distribution. Additionally, we compare our dataset with existing datasets for depth estimation and semantic segmentation in aerial imagery. This comparative analysis aims to underscore the distinctive contributions of DDOS in addressing the challenges posed by thin objects, providing valuable insights into its potential applications and advantages over current datasets in the setting of aerial analysis.

In addition, we introduce new drone-specific metrics tailored specifically to assess depth accuracy in the context of thin object detection and segmentation. These metrics aim to provide a more nuanced and relevant evaluation framework for algorithms operating in drone applications. By accounting for the distinctive challenges posed by thin objects, these metrics offer a more accurate reflection of performance in real-world scenarios, thereby contributing to the advancement of drone technology and safety.

Finally, we present baseline results obtained by applying state-of-the-art algorithms to the DDOS dataset, offering a benchmark for future research in thin object detection and segmentation. The discussion of these baseline results delves into the strengths and limitations of existing

	USF [2]	NE-VBWD [13]	Mid-Air [4]	TartanAir [15]	DDOS (ours)
Data type	<u>Real</u>	<u>Real</u>	<u>Synthetic</u>	<u>Synthetic</u>	<u>Synthetic</u>
Flight Trajectories	<u>86</u>	<u>41</u>	<u>54</u>	<u>1037</u>	<u>340</u>
Frames	<u>6 k</u>	<u>15 k</u>	<u>119 k[†]</u>	<u>1 M</u>	<u>34 k</u>
Labeled frames	<u>3 k</u>	<u>91</u>	<u>119 k[†]</u>	<u>1 M</u>	<u>34 k</u>
Resolution	<u>640 × 480</u>	<u>6576 × 4384</u>	<u>1382 × 512</u>	<u>640 × 480</u>	<u>1280 × 720</u>
Frame rate	<u>25 Hz</u>	<u>2 Hz</u>	<u>25 Hz</u>	-	<u>10 Hz</u>
Environment	<u>Town</u>	<u>Town/Nature</u>	<u>Nature</u>	<u>Various</u>	<u>Town/Nature</u>
Camera motion	<u>Handheld</u>	<u>Helicopter</u>	<u>Drone</u>	<u>Random</u>	<u>Drone</u>
Camera pose	<u>No</u>	<u>No</u>	<u>Yes</u>	<u>Yes</u>	<u>Yes</u>
Optical flow	<u>No</u>	<u>No</u>	<u>No</u>	<u>Yes</u>	<u>Yes</u>
Depth map	<u>No</u>	<u>Sparse</u>	<u>Dense</u>	<u>Dense</u>	<u>Dense</u>
Labeled segmentation	<u>Wires only</u>	<u>Wires only</u>	<u>Yes</u>	<u>No*</u>	<u>Yes</u>
Thin objects	<u>Yes</u>	<u>Yes</u>	<u>No</u>	<u>No*</u>	<u>Yes</u>
Mesh objects	<u>No</u>	<u>No</u>	<u>No</u>	<u>No*</u>	<u>Yes</u>

Table 1. **Comparison between our DDOS dataset and related datasets.** *TartanAir does not include labeled segmentation classes (i.e. each object is assigned to a random unlabeled class, with variations of the same object type in different classes.) The [†] symbol denotes additional variations for the same trajectory exist.

approaches, highlighting opportunities for refinement and innovation.

To summarize, our main contributions are:

- **DDOS Dataset:** We present the Drone Depth and Obstacle Segmentation (DDOS) dataset, specifically designed to tackle the intricate task of detecting and segmenting thin objects.
- **Statistical Analysis and Dataset Comparison:** A comprehensive statistical analysis of DDOS is conducted, shedding light on various key attributes, including object density, spatial distribution, and structural complexity. This analysis is complemented by a meticulous comparison of DDOS against relevant datasets in the field.
- **Drone-Specific Metrics:** Novel drone-specific metrics are introduced, tailored to the nuances of drone applications, particularly in the evaluation of depth accuracy. These metrics offer a refined and specialized framework for assessing algorithmic performance.
- **Baseline Results and Discussion:** Baseline results, achieved through state-of-the-art algorithms applied to the DDOS dataset, are presented. These results serve as a benchmark for future research in thin object detection and segmentation. We engage in a thorough discussion, exploring in-depth insights into the strengths and limitations of the proposed metrics and shedding light on potential avenues for further research and improvement.

2. Related Work

The availability of comprehensive and high-quality datasets for thin object detection is limited.

2.1. Driving datasets

Prominent datasets such as KITTI [6, 10] and Cityscapes [3], while widely utilized in computer vision, are not optimally suited for the specific challenges posed by drone applications.

KITTI, a benchmark dataset for autonomous driving, offers rich annotations for object detection, tracking, and scene understanding. However, its primary focus on road scenes and vehicular scenarios does not align with the nuances of drone navigation. The dataset lacks diversity in the types of thin objects encountered by drones, particularly in scenarios involving cables, wires, and similar structures commonly found in aerial environments. Additionally, KITTI’s distance range and object scale may not fully encompass the variability inherent in drone perspectives, limiting its applicability for developing robust thin object detection models for drone operations.

Similarly, Cityscapes, designed for urban scene understanding, provides detailed semantic segmentation annotations but falls short in addressing the specific challenges faced by drones. In particular, thin objects like wires and cables are not adequately represented. Consequently, models trained on KITTI or Cityscapes may exhibit limitations when applied to drone scenarios, where the detection of slender structures is crucial for safe navigation.

2.2. Wire detection datasets

Some datasets focus solely on wire segmentation, such as USF [2] and NE-VBWD [13]. The USF dataset, a widely used resource, contains just under 6000 images of relatively

low quality, with only around 3000 images featuring wires accompanied by labeled annotations. Notably, the dataset lacks depth information, and the provided ground truth wire annotations are not pixel-accurate. Additionally, wire labels are often either missing or incomplete, as the dataset defines all wires as straight lines, neglecting their potential curvature. This limitation is significant given that wires in real-world scenarios can exhibit substantial curves. Addressing these issues is crucial for advancing the accuracy and applicability of thin object detection models.

NE-VBWD [13] represents a more recent dataset, albeit small, offering both pixel-wise annotations and information regarding the distance to the wires. Notably, this dataset places emphasis on long-range wire detection, making it better suited for manned aircraft rather than drones. Specifically, the majority of wires in the NE-VBWD dataset are situated at a distance of approximately 1 km, with very few within 300 m. This skew towards longer distances is attributed to the dataset’s acquisition via a helicopter, which, due to safety considerations, could not closely approach the wires. Consequently, NE-VBWD proves less useful for drone applications, where the primary concern lies in the detection of wires within the range of 0–100 m, while those beyond this range are of comparatively lesser importance.

2.3. Drone datasets

Both Mid-Air [4] and TartanAir [15] are synthetic datasets generated using Airsim [12]. Mid-Air offers high-resolution images at a high frame rate, with a focus on nature scenes and limited inclusion of man-made objects. In contrast, TartanAir provides numerous trajectories spanning various environments such as towns, cities, nature, indoor settings, and even underwater. However, TartanAir’s segmentation is hindered by assigning objects to random classes, and variations of the same object are placed into different classes. This unhelpful segmentation diminishes the utility of TartanAir for a comprehensive training platform.

Our dataset represents a significant advancement, providing high-resolution images that encompass a rich array of challenging semantic segmentation classes. This diversity spans both intricate man-made environments and the nuanced complexity of natural scenes. By incorporating a broad spectrum of scenarios, our dataset offers a more comprehensive and realistic training platform for algorithms to navigate and interpret varied environments.

To underscore the distinctiveness of our dataset, we present a detailed comparison with other relevant datasets in Table 1. This comparative analysis aims to highlight the unique attributes and advantages of our dataset over existing alternatives, emphasizing its suitability for addressing the intricate task of thin object detection and segmentation in a wide range of real-world scenarios.

3. Dataset Features

We introduce the Drone Depth and Obstacle Segmentation (DDOS) dataset, a synthetic benchmark explicitly designed to tackle the scarcity of annotated real-world data and cater to the challenges of obstacle segmentation and depth estimation from drone perspectives. Comprising 340 unique and diverse drone flights conducted in simulated environments, the DDOS dataset offers a photo-realistic representation of real-world scenarios encountered by drones. This dataset serves as a crucial resource for advancing the field, addressing the limitations associated with the lack of annotated real-world data.

Focusing specifically on thin objects that present significant safety concerns for drone flights, such as cables and wires, DDOS emerges as a valuable resource for the development of algorithms capable of precise segmentation and depth estimation in intricate environments. Each flight in the dataset captures high-resolution images utilizing a monocular camera affixed to the front of the drone. Accompanying these images are corresponding depth maps, pixel-level object segmentation masks, optical flow information, and surface-normals. All image modalities maintain a resolution of 1280×720 , and the depth maps cover a range from 0 to 100 m.

Carefully curated, DDOS is partitioned into training, validation, and testing subsets, encompassing 300, 20, and 20 flights, respectively. Figure 1 provides visual examples, illustrating the diverse classes represented in the dataset, with additional examples shown in Appendix B. This meticulous curation and emphasis on thin objects contribute to the dataset’s efficacy in addressing the intricacies of obstacle segmentation and depth estimation relevant to drone navigation and safety.

DDOS features pixel-wise object segmentation masks with ten distinct classes, allowing for detailed analysis of diverse obstacles and environmental elements. These classes, namely *ultra thin*, *thin*, *small mesh*, *large mesh*, *trees*, *buildings*, *vehicles*, *animals*, *other*, and *background*, provide a comprehensive breakdown. For instance, the *ultra thin* class covers objects like wires and cables, while the *thin* class encompasses streetlights and poles. The *small mesh* class includes objects like fences and nets, and the *large mesh* class involves structures similar to pylons and radio masts. This comprehensive categorization within DDOS serves as a robust resource, facilitating the development and assessment of advanced algorithms specifically tailored to tackle the complex challenges of obstacle segmentation and depth estimation from the unique vantage point of drones.

The synthetic nature of the DDOS dataset overcomes the limitations of scarce annotated real-world data, allowing researchers to systematically explore and compare different approaches in a controlled environment. By leveraging this dataset, researchers can advance the field of drone

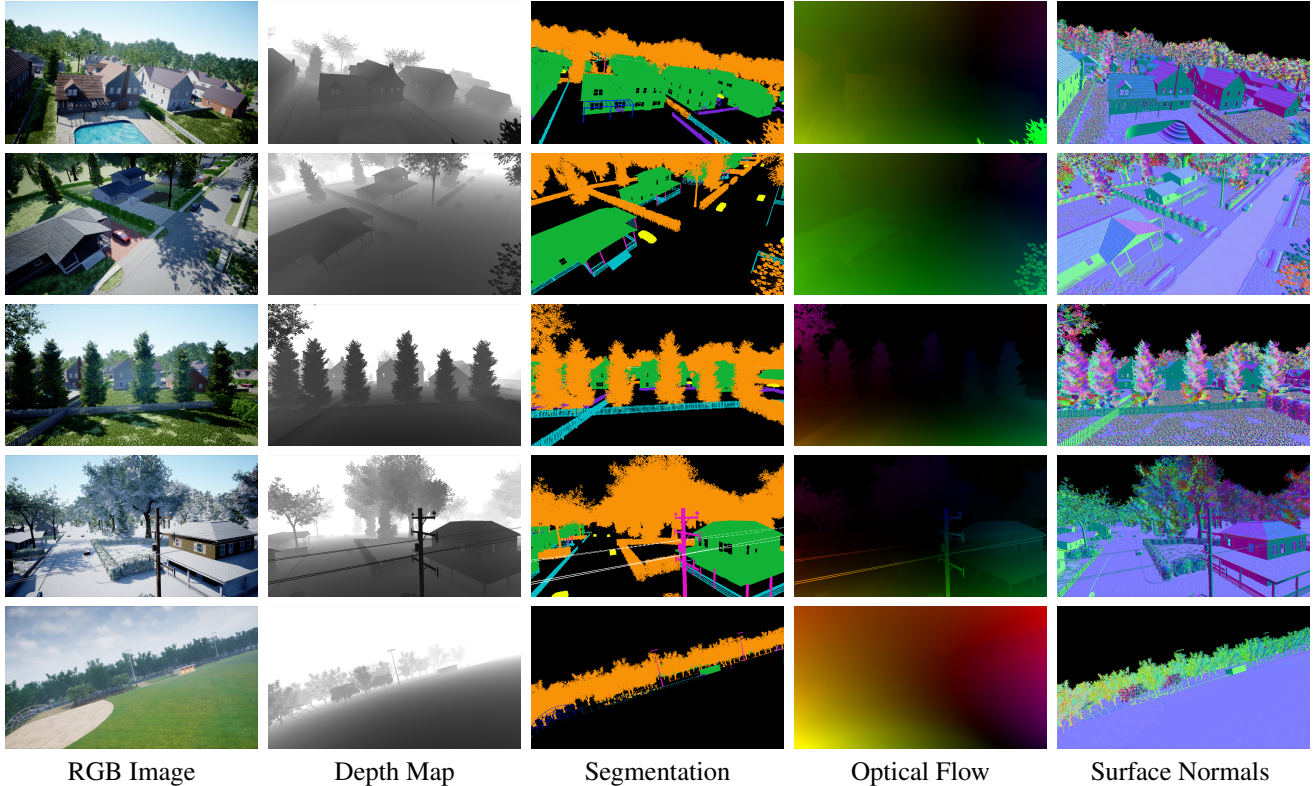


Figure 1. **Examples from our DDOS dataset.** First column: single RGB image frame from drone flight. Second column: corresponding depth map (0–100 m). Third column: pixel-wise semantic segmentation. Fourth column: optical flow. Fifth column: surface normals. Best viewed on computer and zoomed in.

vision, developing innovative solutions to address the challenges of obstacle segmentation and depth estimation. Ultimately, DDOS aims to enhance the safety and efficiency of drone operations by facilitating the development of robust algorithms capable of accurately detecting and navigating around thin objects, such as cables and wires, which are critical for ensuring the safety of drone flights.

4. Data Generation

The images in DDOS are generated using AirSim[12], a drone simulator. DDOS is composed of two environments that mimic real-world scenarios. The first environment resembles a small suburban town, featuring dense trees and numerous power lines, replicating the challenges faced during drone flights in residential areas. The second environment represents a park setting, incorporating elements such as a football field with floodlights, a beach volleyball court, dense trees as well as office buildings. These environments collectively offer diverse obstacles and structures, allowing researchers to develop and evaluate algorithms capable of addressing the complexities associated with different real-world environments. By encompassing characteristics like dense tree coverage, power lines and varying weather con-

ditions, such as snow cover, the dataset provides a comprehensive platform for advancing obstacle segmentation and depth estimation algorithms for safe and effective drone flights.

Flight trajectories To construct each flight trajectory, a random starting location (x_0, y_0, z_0) , within the environment bounds is selected. Subsequently, multiple intermediate target points (x_t, y_t, z_t) are generated within predefined relative bounding boxes, dictating the areas to which the drone navigates. Flight characteristics, are varied across different flights, providing diversity in the dataset. During each flight, observations are recorded at a rate of 10 Hz for a duration of 10 seconds. These observations encompass a rich set of data, including images, depth maps, pixel-wise object segmentation, optical flow, and surface-normals.

Collision avoidance In order to promote relatively safe flight paths, we developed a dynamic obstacle detection algorithm to modify intermediate targets in response to potential collision risks. This algorithm utilizes the most recent ground truth depth map obtained during the recorded flight observations. By empirically determining a thresh-

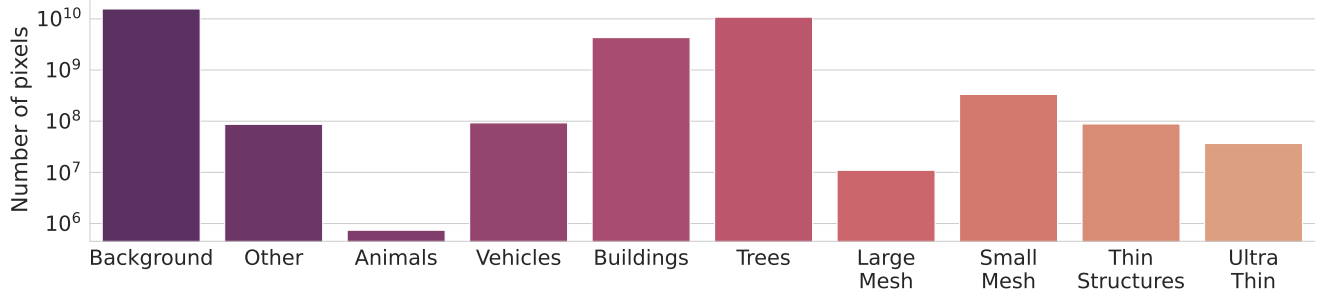


Figure 2. **Distribution of class labels within DDOS.** DDOS effectively captures the presence of various thin object classes, which are characterized by a relatively sparse distribution of pixels within each image. Despite their limited pixel coverage, these thin object classes are well-represented in DDOS, ensuring comprehensive coverage and enabling robust training and evaluation of algorithms specifically designed to address the challenges posed by such objects.

old, objects that are deemed too close trigger updates to the intermediate targets. The updated targets are strategically adjusted based on the detected obstacle’s location, causing the drone to navigate away from the identified collision risk. This obstacle avoidance approach is not flawless, especially when dealing with thin objects, occasional collisions resulting in crashes still occur. In such cases, the observations associated with the crash event are discarded, and the flight process is restarted to ensure data integrity. It is important to note, the collision avoidance mechanism is purposefully designed to be lax, as near misses and even minor crashes can offer valuable data points for training purposes.

Post-processing To uphold the overall integrity of the dataset and exclude instances of undesired behavior, additional validation criteria are applied after flight generation. These criteria serve to filter out scenarios where the drone becomes stuck or encounters unusual situations, such as becoming entangled in trees. By incorporating these post-flight validation steps, the dataset ensures that the collected observations reflect reliable and meaningful flight behaviors, enabling robust algorithm training and evaluation.

Data augmentation We do not augment the dataset with additional transformations or modifications, such as chromatic aberration, added lens flares, corruption, or noise, during the data collection process. The decision to exclude these augmentation techniques at the initial phase ensures that the dataset remains in its original state, preserving the inherent characteristics and properties of the collected data. Instead, we provide the flexibility to incorporate these augmentation techniques at a later stage, if deemed necessary, during algorithm development and evaluation.

Weather Incorporating diverse weather conditions, such as snow cover and wet roads, is crucial for enhancing the robustness of computer vision models, particularly in the

context of autonomous systems and transportation. Adverse weather introduces challenges like reduced visibility and altered surface characteristics, which significantly impact the performance of vision-based algorithms. Snow cover, for instance, introduces high reflectivity and obscures road markings, demanding algorithms capable of adapting to these dynamic conditions. Similarly, wet roads can lead to glare and reflections, posing challenges for accurate object detection and scene understanding. By including such weather scenarios in datasets, researchers can develop and evaluate models that demonstrate resilience in real-world, dynamic environments, ultimately advancing the reliability of computer vision systems across various weather conditions.

5. Dataset Statistics

In this section, we provide a comprehensive analysis of key properties inherent in the DDOS dataset. The visual representation in Figure 2 vividly illustrates the distribution of annotations across diverse classes within DDOS. Significantly, the dataset adeptly captures and represents various classes of thin objects, even when these objects occupy a relatively small number of pixels in each image. This nuanced representation ensures that DDOS offers a substantial and well-balanced dataset for thin object classes. This richness in diversity is paramount for facilitating thorough analysis, robust algorithm training, and effective evaluation, particularly in addressing the challenges associated with thin objects in real-world scenarios. The carefully crafted distribution of classes within DDOS contributes to its utility as a reliable benchmark for advancing the capabilities of algorithms designed for thin object detection and segmentation.

Continuing our exploration, we delve into the examination of pitch and roll angles recorded during the flights. As depicted in Figure 3, the visualization illustrates a broad spectrum of pitch and roll angles, highlighting substan-

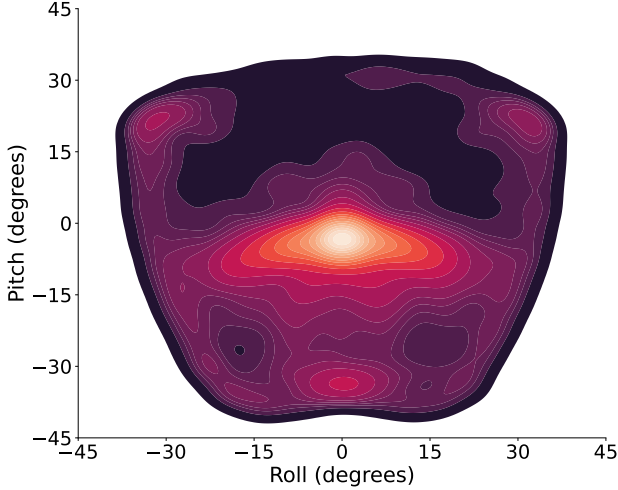


Figure 3. **Distribution of pitch and roll angles.** The colors represent the intensity levels, with warmer colors indicating higher occurrences. Flight characteristics vary between each flight, as highlighted by the diverse pitch and roll degrees. The pitch is negative when the drone is accelerating forward and positive when braking or to go backwards. Emergency braking is often accompanied with a sharp turn, either to the left or to the right.

tial variations in the drone’s orientation throughout the dataset. Remarkably, despite the drone’s predominant forward movement in the dataset, the recorded angles exhibit noteworthy diversity. This diversity in orientation contributes invaluable viewing perspectives, offering a holistic evaluation of algorithms under diverse flight conditions. The extensive distribution of pitch and roll angles underscores the DDOS dataset’s capacity to emulate real-world scenarios, where drones navigate through varying pitch and roll angles. This feature ensures the dataset’s efficacy in training and assessing algorithms to perform reliably across a spectrum of orientation challenges encountered during drone flights.

To gain an intuitive understanding of the spatial distribution of flight paths within a singular environment, we visually present a subset of the recorded trajectories in Figure 4. The depicted flight paths showcase a diverse array of patterns, ranging from sharp turns and straight lines to curved trajectories. These variations authentically capture the complexity and dynamic nature of the simulated environments. Furthermore, an overhead view of the relative flight paths, presented in Figure 5, offers a normalized perspective with a common starting point and direction. This visualization emphasizes the diverse flight trajectories and patterns observed across individual flights, providing a comprehensive overview of the spatial dynamics inherent in the DDOS dataset. Such a representation is instrumental in offering insights into the intricate navigation challenges that algo-

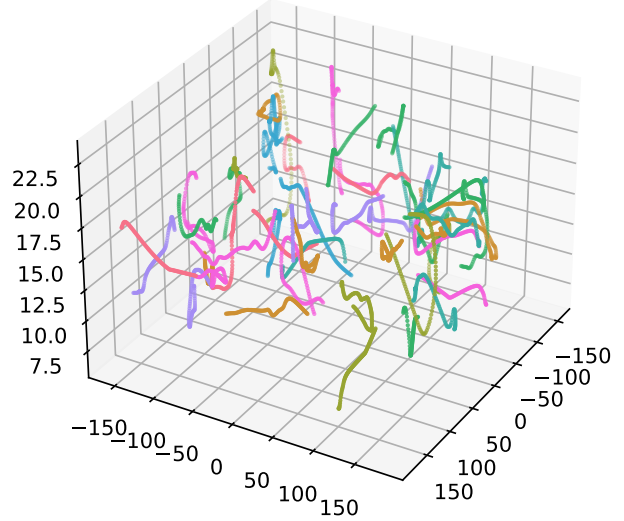


Figure 4. **Illustrated flight paths.** The figure presents a collection of 50 randomly selected flight paths conducted within the same environment. The paths exhibit significant variations in trajectory, highlighting the diverse nature of drone flights.

gorithms must address, reinforcing the dataset’s efficacy in training and evaluating models under diverse and realistic conditions.

Expanding our analysis, we delve into the distributions of altitude and speed during the flights, along with the distribution of depth recorded in the depth maps, as illustrated collectively in Figure 6. Examining the altitude distribution reveals that the drone operates at varying heights, encompassing low-level flights near the ground to higher altitudes. The distribution of speed elucidates a spectrum of velocities encountered during the flights, showcasing diverse flight behaviors and maneuvering speeds. Moreover, the depth distribution offers insights into the range and distribution of depth values recorded in the depth maps, shedding light on the variations in perceived depth across the dataset. This multifaceted exploration of altitude, speed, and depth distributions provides a comprehensive understanding of the dynamic spatial characteristics inherent in the DDOS dataset, crucial for informing the development and evaluation of algorithms designed to navigate and perceive diverse environments encountered by drones.

6. Depth metrics

We propose a novel set of depth metrics specifically tailored for drone applications, namely the absolute relative depth estimation error for each distinct class. To illustrate, we introduce the absolute relative depth error metric for the *ultra thin* class within the DDOS dataset. This metric quantifies the accuracy of depth estimation specifically for objects classified as *ultra thin* in the DDOS dataset.

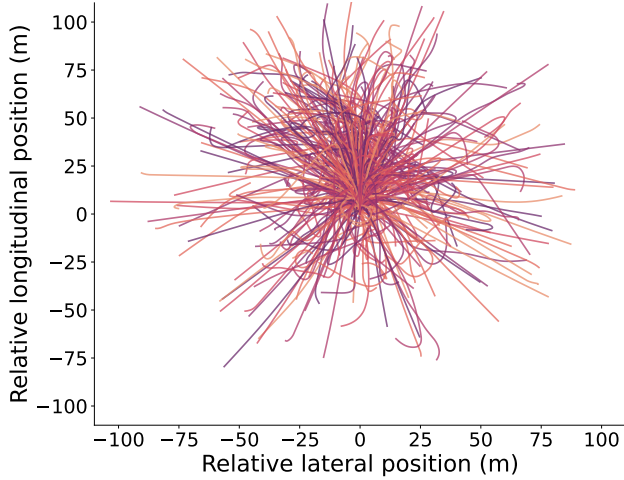


Figure 5. **Overhead view of relative flight paths with a normalized starting point.** In this visualization the starting location and direction have been normalized to highlight the various relative shapes of the flight paths. The actual starting locations are randomly initialized, as shown in Figure 4.

$$AbsRel_{ultra\ thin} = \frac{1}{N_{ultra\ thin}} \sum_{i=1}^{N_{ultra\ thin}} \left| \frac{d_i - \hat{d}_i}{d_i} \right| \quad (1)$$

In this formula, $AbsRel_{ultra\ thin}$ represents the absolute relative depth estimation error for the *ultra thin* class. $N_{ultra\ thin}$ denotes the total number of samples in the *ultra thin* class. d_i and \hat{d}_i represent the ground truth depth and estimated depth for the i -th pixel sample, respectively. The formula calculates the average absolute relative difference between the ground truth and estimated depths for all samples in the *ultra thin* class.

By evaluating the absolute relative depth error for this class, we can assess the performance of depth estimation algorithms in accurately capturing the depth information of ultra thin objects, such as wires and cables. The introduction of class-specific depth metrics enables a more comprehensive evaluation of depth estimation algorithms tailored to the unique challenges posed by different object categories encountered in drone views.

Trivially, extending this approach to all classes, the general formula for class-specific depth metrics becomes:

$$AbsRel_{class} = \frac{1}{N_{class}} \sum_{i=1}^{N_{class}} \left| \frac{d_i - \hat{d}_i}{d_i} \right| \quad (2)$$

By assessing the absolute relative depth error for each class, we gain insights into the performance of depth estimation algorithms in accurately capturing the depth information of specific objects, such as wires and cables. The incorporation of class-specific depth metrics facilitates a more

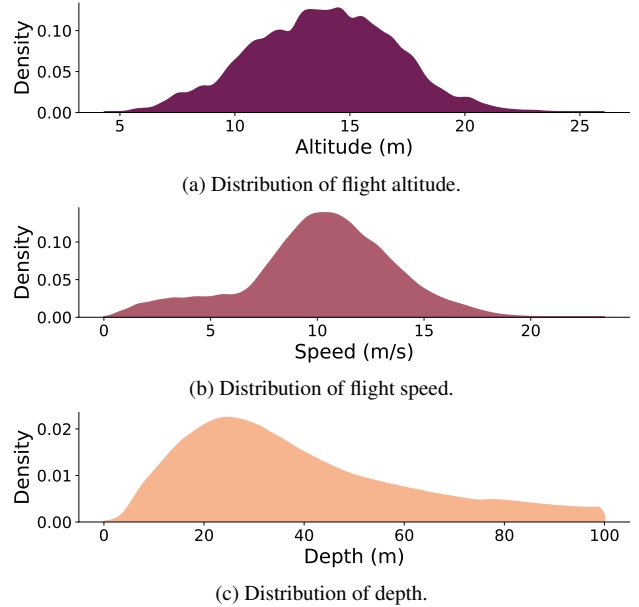


Figure 6. **Distributions of altitude, speed and depth.** The distributions show variation across flights. Depth over 100 m is ignored.

nuanced evaluation of depth estimation algorithms, addressing the unique challenges presented by various object categories encountered in drone views.

7. Baselines

We employ a comprehensive set of metrics to rigorously evaluate the effectiveness of our baselines. These metrics include fundamental measures such as accuracy under the threshold ($\delta_i < 1.25^i$, $i = 1, 2, 3$), which assesses the model’s performance within certain proximity thresholds. Additionally, we consider common metrics like mean absolute relative error (AbsRel), mean squared relative error (SqRel), root mean squared error (RMSE), root mean squared log error (RMSElog), and mean log10 error (log10). These metrics provide insights into the accuracy and precision of our depth estimation. To further enhance our evaluation, we integrate the scale-invariant logarithmic error (SILog).

Moreover, in pursuit of a more nuanced evaluation, we leverage our newly proposed suite of metrics known as mean absolute relative class error metrics ($AbsRel_{class}$). This suite is tailored to assess the performance of our methods at a finer class level, offering a more detailed understanding of their capabilities. This diverse array of metrics ensures a thorough assessment of the selected baselines.

We utilise three different baselines, BinsFormer [8], SimIPU [7] and DepthFormer [9]. BinsFormer proposes a novel framework for monocular depth estimation by formulating it as a classification-regression task, employing

Model	$\delta_1 \uparrow$	$\delta_2 \uparrow$	$\delta_3 \uparrow$	AbsRel \downarrow	RMSE \downarrow	log10 \downarrow	RMSElog \downarrow	SILog \downarrow	SqRel \downarrow
BinsFormer [8]	0.807	0.930	0.970	0.153	7.354	0.061	0.212	19.529	1.848
SimIPU [7]	0.811	0.931	0.969	0.149	6.366	0.056	0.206	19.470	1.770
DepthFormer [9]	0.873	0.957	0.981	0.108	5.761	0.045	0.171	16.542	1.119

Table 2. This table presents the performance metrics of three baselines, BinsFormer, SimIPU, and DepthFormer, in monocular depth estimation. Notably, DepthFormer outperforms the other baselines across all metrics, showcasing its superior performance in accurately estimating depth. The arrows indicate desired outcome.

Model	Ultra Thin	Thin Structures	Small Mesh	Large Mesh	Trees	Buildings	Vehicles	Animals	Other	Background
BinsFormer [8]	0.686	0.248	0.149	0.206	0.251	0.156	0.153	0.139	0.159	0.108
SimIPU [7]	0.664	0.280	0.157	0.232	0.279	0.188	0.165	0.149	0.181	0.097
DepthFormer [9]	0.634	0.228	0.118	0.187	0.189	0.123	0.138	0.115	0.154	0.067

Table 3. Class-wise Absolute Relative Depth Errors. Each baseline’s performance is evaluated, with lower values indicating better performance. DepthFormer consistently achieves the lowest errors across all classes. All methods severely struggle for the Ultra thin class.

a transformer [14] decoder to generate adaptive bins [1]. SimIPU introduces a pre-training strategy for spatial-aware visual representation, utilizing point clouds for improved spatial information in contrastive learning. DepthFormer addresses supervised monocular depth estimation by leveraging a transformer for global context modeling, incorporating an additional convolution branch, and introducing a hierarchical aggregation module. All three baselines demonstrate superior performance in monocular depth estimation compared to state-of-the-art methods across various datasets.

The evaluation of depth estimation baselines is shown in table 2. DepthFormer emerges as the standout performer, consistently surpassing its counterparts in accuracy under different thresholds, mean absolute relative error, and other key metrics. The success of *DepthFormer* can be attributed to its innovative approach, leveraging a transformer for global context modeling, incorporating additional convolutional branches, and introducing hierarchical aggregation modules. These features enhance both local and global information processing, resulting in superior depth estimation capabilities.

The scrutiny of our novel class-specific depth metrics, as delineated in table 3, unveils the challenges inherent in accurately estimating the depth of specific object classes across all methods under consideration. Notably, the ultra-thin class emerges as a particularly formidable challenge, as evidenced by the discernible difficulties encountered by all methods in providing precise depth estimations for this category. The observed limitations in accurately capturing the depth of ultra-thin objects underscore the complexities associated with fine-grained depth estimation, warranting further investigation and refinement of methodologies. This underscores the necessity for methodological advancements

that specifically address drone setting and the intricacies of ultra-thin object depth estimation, signaling a potential avenue for future research and algorithmic refinement. To further highlight these challenges, we present qualitative examples in Appendix C for illustrative purposes.

8. Conclusion

Accurate depth and semantic segmentation play pivotal roles in diverse computer vision applications, from autonomous navigation to surveillance. However, the shortage of annotated real-world aerial datasets poses a formidable challenge, hindering the development and evaluation of robust models. To address these challenges, this work introduces DDOS, a synthetic dataset tailored for depth and semantic segmentation tasks in aerial views. Leveraging AirSim [12], DDOS serves as a crucial resource for model training, particularly in scenarios where real-world annotated data is scarce. Furthermore, the introduction of novel drone-specific metrics for depth accuracy is a noteworthy contribution, promising to advance the evaluation standards for models operating in drone-specific scenarios.

Inaccuracies in detecting elements such as cables and wires pose significant risks, warranting specialized attention in model development. DDOS and drone-specific metrics introduced in this work not only address current limitations but also pave the way for future advancements in computer vision for aerial views. The tailored metrics offer a nuanced evaluation framework, ensuring that models are proficient not only in general scenarios but also in the intricacies of drone-specific contexts. As such, this research contributes to the broader landscape of safety-conscious drone technologies and fosters advancements in computer vision research for aerial applications.

References

- [1] Shariq Farooq Bhat, Ibraheem Alhashim, and Peter Wonka. Adabins: Depth estimation using adaptive bins. In *Proceedings of the IEEE/CVF Conference on Computer Vision and Pattern Recognition*, pages 4009–4018, 2021. 8
- [2] Joshua Candamo, Rangachar Kasturi, Dmitry Goldgof, and Sudeep Sarkar. Detection of Thin Lines using Low-Quality Video from Low-Altitude Aircraft in Urban Settings. *IEEE Transactions on Aerospace and Electronic Systems*, 45(3): 937–949, 2009. 2
- [3] Marius Cordts, Mohamed Omran, Sebastian Ramos, Timo Rehfeld, Markus Enzweiler, Rodrigo Benenson, Uwe Franke, Stefan Roth, and Bernt Schiele. The cityscapes dataset for semantic urban scene understanding. In *Proceedings of the IEEE Conference on Computer Vision and Pattern Recognition (CVPR)*, 2016. 2
- [4] Michael Fonder and Marc Van Droogenbroeck. Mid-air: A multi-modal dataset for extremely low altitude drone flights. In *Proceedings of the IEEE/CVF conference on computer vision and pattern recognition workshops*, pages 0–0, 2019. 1, 2, 3
- [5] Timnit Gebru, Jamie Morgenstern, Briana Vecchione, Jennifer Wortman Vaughan, Hanna Wallach, Hal Daumé Iii, and Kate Crawford. Datasheets for datasets. *Communications of the ACM*, 64(12):86–92, 2021. 10
- [6] Andreas Geiger, Philip Lenz, and Raquel Urtasun. Are we ready for autonomous driving? the kitti vision benchmark suite. In *2012 IEEE conference on computer vision and pattern recognition*, pages 3354–3361. IEEE, 2012. 2
- [7] Zhenyu Li, Zehui Chen, Ang Li, Liangji Fang, Qinrong Jiang, Xianming Liu, Junjun Jiang, Bolei Zhou, and Hang Zhao. Simipu: Simple 2d image and 3d point cloud unsupervised pre-training for spatial-aware visual representations. In *Proceedings of the AAAI Conference on Artificial Intelligence*, pages 1500–1508, 2022. 7, 8, 15
- [8] Zhenyu Li, Xuyang Wang, Xianming Liu, and Junjun Jiang. Binsformer: Revisiting adaptive bins for monocular depth estimation. *arXiv preprint arXiv:2204.00987*, 2022. 7, 8, 15
- [9] Zhenyu Li, Zehui Chen, Xianming Liu, and Junjun Jiang. Depthformer: Exploiting long-range correlation and local information for accurate monocular depth estimation. *Machine Intelligence Research*, pages 1–18, 2023. 7, 8, 15
- [10] Moritz Menze and Andreas Geiger. Object scene flow for autonomous vehicles. In *Proceedings of the IEEE conference on computer vision and pattern recognition*, pages 3061–3070, 2015. 2
- [11] Payal Mittal, Raman Singh, and Akashdeep Sharma. Deep learning-based object detection in low-altitude uav datasets: A survey. *Image and Vision computing*, 104:104046, 2020. 1
- [12] Shital Shah, Debadeepta Dey, Chris Lovett, and Ashish Kapoor. Airsim: High-fidelity visual and physical simulation for autonomous vehicles. In *Field and Service Robotics*, 2017. 3, 4, 8, 11
- [13] Adam Stambler, Gary Sherwin, and Patrick Rowe. Detection and Reconstruction of Wires Using Cameras for Aircraft Safety Systems. In *2019 International Conference on Robotics and Automation (ICRA)*, pages 697–703, 2019. ISSN: 1050-4729. 2, 3
- [14] Ashish Vaswani, Noam Shazeer, Niki Parmar, Jakob Uszkoreit, Llion Jones, Aidan N Gomez, Łukasz Kaiser, and Illia Polosukhin. Attention is all you need. *Advances in neural information processing systems*, 30, 2017. 8
- [15] Wenshan Wang, Delong Zhu, Xiangwei Wang, Yaoyu Hu, Yuheng Qiu, Chen Wang, Yafei Hu, Ashish Kapoor, and Sebastian Scherer. Tartanair: A dataset to push the limits of visual slam. In *2020 IEEE/RSJ International Conference on Intelligent Robots and Systems (IROS)*, pages 4909–4916. IEEE, 2020. 1, 2, 3
- [16] World Economic Forum Global Future Council on Human Rights 2016–2018. How to prevent discriminatory outcomes in machine learning. <https://www.weforum.org/whitepapers/how-to-prevent-discriminatory-outcomes-in-machine-learning>, 2018. 10

DDOS: The Drone Depth and Obstacle Segmentation Dataset

Supplementary Material

A. Datasheet

In light of the growing recognition of the pivotal role that datasets play in shaping the behavior and outcomes of machine learning models, this section adheres to the framework proposed in the *Datasheets for Datasets* paper [5]. Acknowledging the potential consequences of mismatches between training or evaluation datasets and real-world deployment contexts, as well as the risk of perpetuating societal biases within machine learning models, we embrace the call for increased transparency and accountability in documenting the provenance, creation, and use of machine learning datasets [16]. By adopting this standardized reporting scheme, we aim to provide a comprehensive understanding of our dataset’s motivation, composition, collection process, and recommended uses. This adherence to the datasheets for datasets framework aligns with the broader objective of enhancing transparency, mitigating biases, fostering reproducibility, and aiding researchers and practitioners in selecting datasets tailored to their specific tasks. In the following subsections, we systematically address the key questions outlined in the datasheets for datasets, providing a thorough account of our dataset’s characteristics and attributes.

A.1. Motivation

For what purpose was the dataset created? The Drone Depth and Obstacle Segmentation (DDOS) dataset, was created to address the limitations posed by the scarcity of annotated aerial datasets, specifically for training and evaluating models in depth and semantic segmentation tasks. The primary objective is to focus on the detection and segmentation of thin objects like wires, cables, and fences in aerial views, which are critical for ensuring the safe operation of drones. The dataset aims to fill the gap in existing datasets that predominantly concentrate on common objects and lack representation of fine spatial characteristics of thin objects.

Who created the dataset and on behalf of which entity?

The dataset was created by Benedikt Kolbeinsson and Kryszian Mikolajczyk.

A.2. Composition

What do the instances that comprise the dataset represent? The instances in the dataset represent individual drone flights which are composed of sequences of observations (images, depth maps, segmentation, etc.) captured during each flight.

How many instances are there in total? The dataset consists of a total of 340 drone flights, and each flight comprises 100 sequential observations. Therefore, there are a total of 34,000 observations ($340 \text{ flights} \times 100 \text{ observations per flight}$).

Does the dataset contain all possible instances or is it a sample (not necessarily random) of instances from a larger set? No, there exists many more possible flight paths in the environments used as well as in other environments.

What data does each instance consist of? Each flight consists of 100 sequential observations, comprising of a high-resolution image captured by a monocular camera affixed to the front of the drone, corresponding depth maps, pixel-level object segmentation masks, optical flow information and surface normals. As well as coordinates, pose and speed information and environment information including weather. All image modalities maintain a resolution of 1280×720 , and the depth maps cover a range from 0 to 100 meters.

Is there a label or target associated with each instance?

Yes, DDOS features pixel-wise object segmentation masks with ten distinct classes, allowing for detailed analysis of diverse obstacles and environmental elements. These classes are: *ultra thin*, *thin*, *small mesh*, *large mesh*, *trees*, *buildings*, *vehicles*, *animals*, *other*, and *background*. For instance, the *ultra thin* class covers objects like wires and cables, while the *thin* class encompasses streetlights and poles. The *small mesh* class includes objects like fences and nets, and the *large mesh* class involves structures similar to pylons and radio masts. In addition, corresponding depth maps, optical flow information and surface normals are included.

Is any information missing from individual instances?

No.

Are relationships between individual instances made explicit? Yes, the flight coordinates are available.

Are there recommended data splits? Yes, the dataset is partitioned into training, validation, and testing subsets, encompassing 300, 20, and 20 flights, respectively.

Are there any errors, sources of noise, or redundancies in the dataset? The data is simulated and no artificial noise is added.

Is the dataset self-contained, or does it link to or otherwise rely on external resources? Yes, DDOS is self-contained.

Does the dataset contain data that might be considered confidential? No.

Does the dataset contain data that, if viewed directly, might be offensive, insulting, threatening, or might otherwise cause anxiety? No.

A.3. Collection Process

How was the data associated with each instance acquired? The data was acquired through simulated drone flights using AirSim [12], a drone simulator.

What mechanisms or procedures were used to collect the data? DDOS was generated using AirSim and data was saved using built-in APIs.

If the dataset is a sample from a larger set, what was the sampling strategy? During the simulation process, flights with severe crashes were discarded.

Who was involved in the data collection process? Data collection scripts were written by Benedikt Kolbeinsson.

Over what timeframe was the data collected? The simulation process took two days.

Were any ethical review processes conducted? No.

A.4. Preprocessing / cleaning / labeling

Was any preprocessing / cleaning / labeling of the data done? During the simulation, labels such as depth and semantic segmentation are automatically recorded. Flights with severe crashes were discarded.

Was the “raw” data saved in addition to the preprocessed / cleaned / labeled data? The processed data is a lossless function of the raw data. The only removed data are flights with severe crashes and are not saved.

Is the software that was used to preprocess / clean / label the data available? Yes, AirSim is open source.

A.5. Uses

Has the dataset been used for any tasks already? No.

Is there a repository that links to any or all papers or systems that use the dataset? No.

What (other) tasks could the dataset be used for? DDOS is valuable for training and evaluating algorithms related to obstacle and object segmentation, depth estimation, and drone navigation.

Is there anything about the composition of the dataset or the way it was collected and preprocessed / cleaned / labeled that might impact future uses? No.

Are there tasks for which the dataset should not be used? Yes, DDOS should not be used for malicious purposes.

A.6. Distribution

Will the dataset be distributed to third parties outside of the entity on behalf of which the dataset was created? Yes, DDOS is hosted on Hugging Face and is openly available:

huggingface.co/datasets/benediktcol/DDOS

How will the dataset be distributed? DDOS is openly available on Hugging Face:

huggingface.co/datasets/benediktcol/DDOS

When will the dataset be distributed? On publication of this paper.

Will the dataset be distributed under a copyright or other intellectual property (IP) license, and/or under applicable terms of use (ToU)? Yes, DDOS is openly licensed under [CC BY-NC 4.0](https://creativecommons.org/licenses/by-nc/4.0/).

Have any third parties imposed IP-based or other restrictions on the data associated with the instances? No.

Do any export controls or other regulatory restrictions apply to the dataset or to individual instances? No.

A.7. Maintenance

Who will be supporting / hosting / maintaining the dataset? DDOS is hosted on Hugging Face

How can the owner / curator / manager of the dataset be contacted? Contact can be made on Hugging Face: huggingface.co/datasets/benediktkol/DDOS

Is there an erratum? No.

Will the dataset be updated? There is no current plan to augment the dataset.

If the dataset relates to people, are there applicable limits on the retention of the data associated with the instances? Not applicable.

Will older versions of the dataset continue to be supported / hosted / maintained? Yes.

If others want to extend / augment / build on / contribute to the dataset, is there a mechanism for them to do so? There is no specific mechanism for others to extend / augment / build on / contribute to the dataset.

B. Additional Examples

We present additional frames from DDOS in Figures 7 and 8. To accentuate finer details, the visualizations focus solely on the RGB image alongside its corresponding depth map and semantic segmentation. The showcased frames exhibit diverse variations in perspective, encompassing different types of vegetation, architectural structures, and meteorological phenomena such as snow cover. Figure 8 highlights examples with instances belonging to the *Ultra thin* class, as well as examples from the *Thin structures* and *Small mesh* classes.

DDOS, serves as a comprehensive resource for the research community, particularly in the domains of depth estimation and segmentation. Its utility is especially evident in scenarios involving aerial perspectives, as encountered by drones, offering valuable insights for discerning thin objects within the visual field.

C. Qualitative Results

In this section, we present qualitative results obtained from the baseline models, as illustrated in Figure 9. A visual inspection reveals substantial similarities among the baseline models in their overall performance. Notably, each struggles when predicting the maximum depth, indicating a shared limitation across the evaluated approaches.

However, a more detailed analysis unveils distinct challenges faced by the BinsFormer model, particularly in its handling of the sky and clouds. This model exhibits a pronounced difficulty, often misjudging the proximity of clouds, thereby leading to inaccurate predictions. On the other hand, all models demonstrate commendable proficiency in accurately predicting thin structures, exemplified by floodlights and electrical poles. Regrettably, a notable deficiency emerges collectively across all models concerning *Ultra thin* objects, specifically wires, where each model experiences a substantial failure.

This observed limitation underscores the exigency for DDOS. It becomes evident that current state-of-the-art techniques are ill-equipped to effectively address the intricacies associated with ultra-thin objects, emphasizing the imperative for novel methodologies. The introduction of the DDOS dataset is motivated by the need to provide a dedicated resource for advancing research in ultra-thin object depth estimation and segmentation, acknowledging the scarcity of suitable data for addressing this specific challenge.

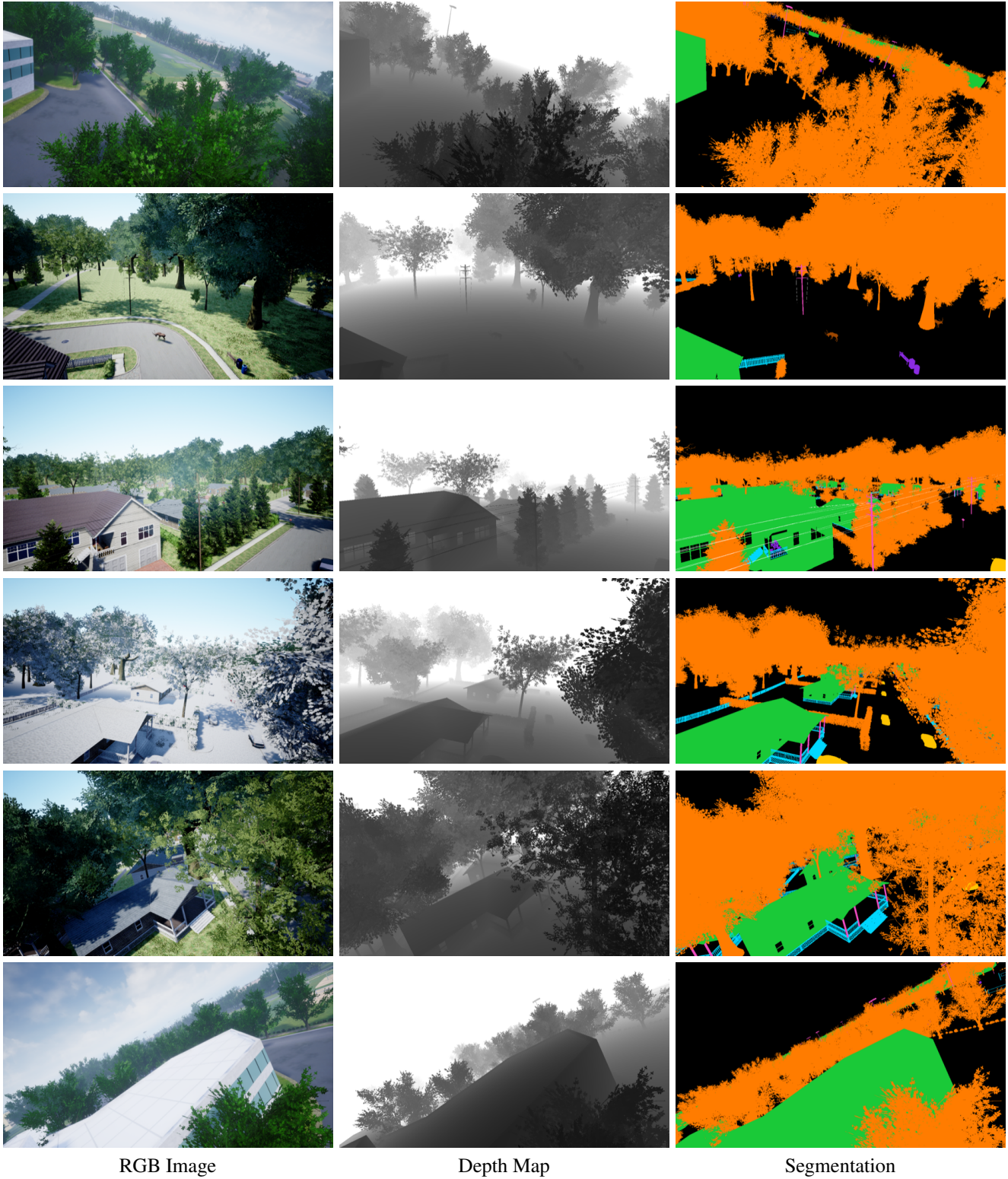


Figure 7. **Diverse perspectives in DDOS.** A selection of frames showcasing various aerial views from DDOS. The RGB image is presented alongside its corresponding depth map and semantic segmentation. Noteworthy details include different types of vegetation, architectural structures, and meteorological phenomena such as snow cover. Optical flow and surface normals, although available, are not displayed in this visualization. It is recommended to view on a computer and zoom in to accentuate finer features.

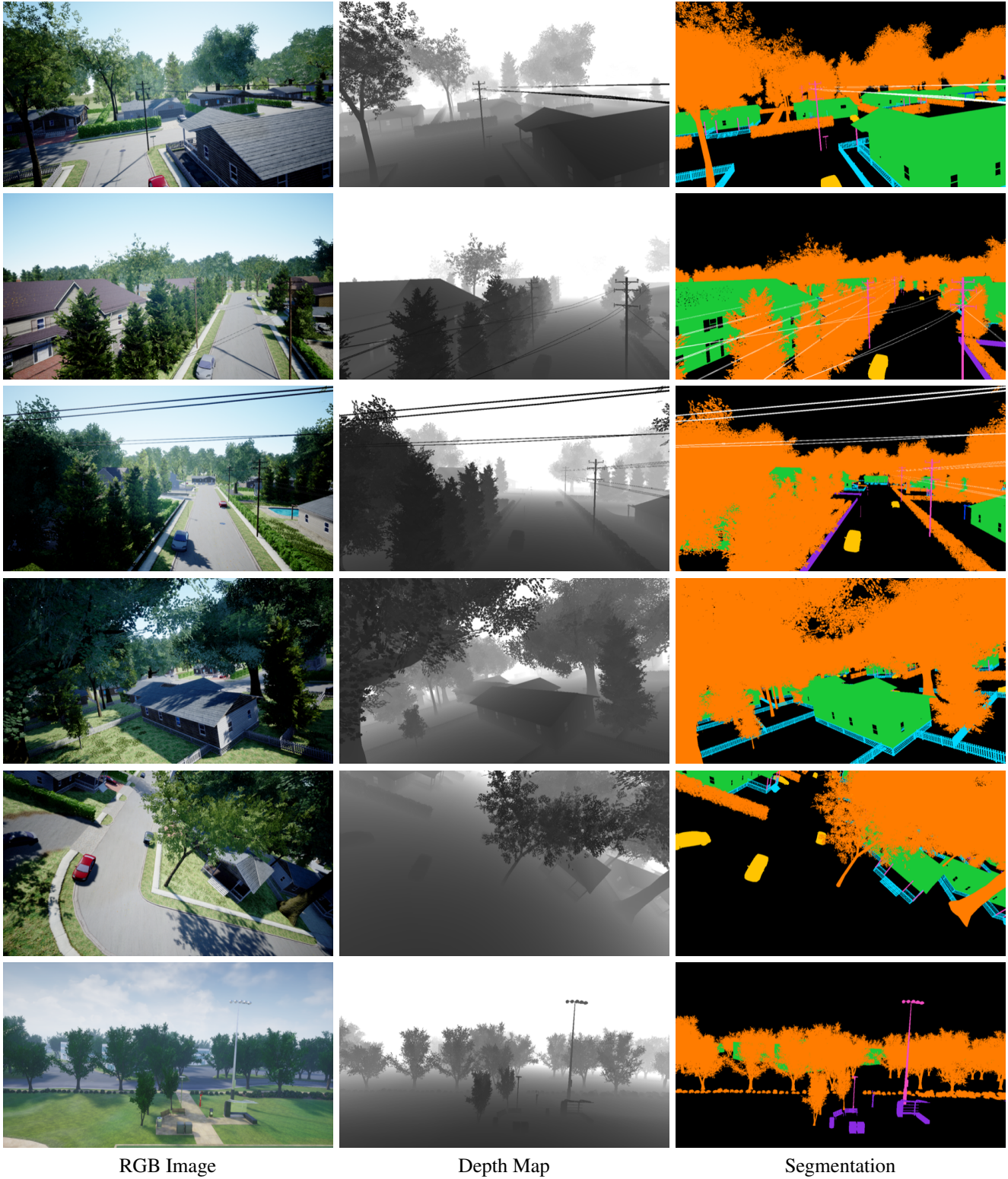


Figure 8. **Highlighting challenging scenarios in DDOS.** These examples emphasize instances from the *Ultra thin*, *Thin structures*, and *Small mesh* classes within DDOS. The RGB image, accompanied by its corresponding depth map and semantic segmentation, provides insight into scenarios encountered by drones. While optical flow and surface normals are part of the dataset, they are not shown in this visualization. For optimal viewing, it is recommended to use a computer and zoom in to explore intricate details.

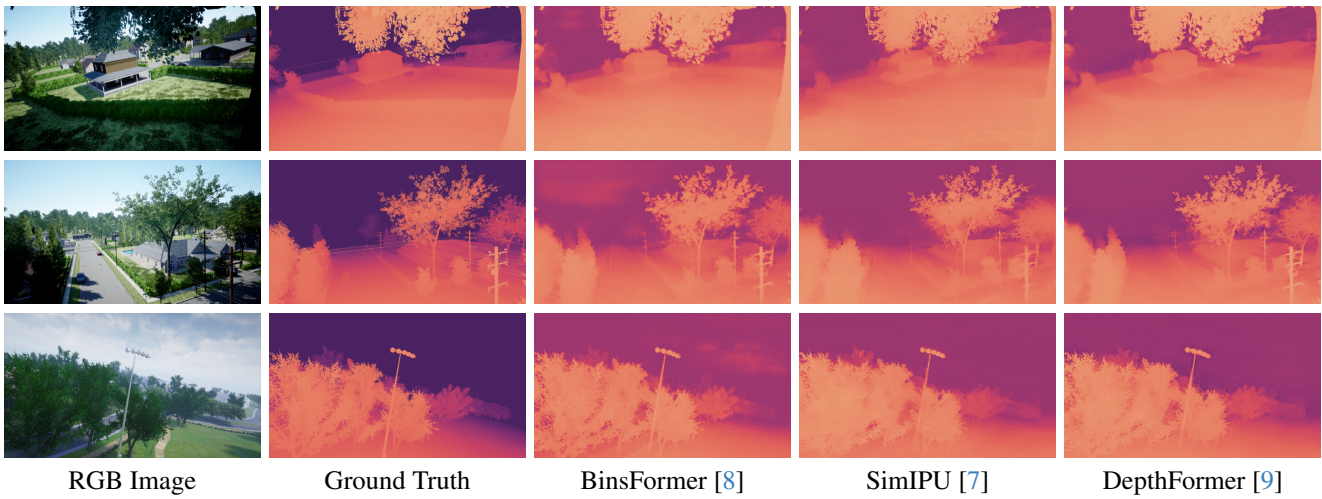


Figure 9. **Depth estimation performance of baselines.** This qualitative assessment underscores the challenges faced by state-of-the-art methods in accurately estimating depth, particularly for the *Ultra thin* class. The middle row prominently showcases the shared difficulty encountered by all methods. Additionally, the top row illustrates the struggle in capturing the *Ultra thin* class when it appears in the distant background—a consistent issue across all methods, but most conspicuous in the middle row. This emphasizes the intricate nature of accurately discerning depth for such instances.